

Theoretical modeling of antiferrodistortive phase transition for SrTiO₃ ultrathin films

E. Blokhin,^{1,*} R. A. Evarestov,^{1,2} D. Gryaznov,^{1,3} E. A. Kotomin,^{1,3} and J. Maier¹

¹Max Planck Institute for Solid State Research, Stuttgart, Germany

²Department of Quantum Chemistry, St. Petersburg State University, Peterhof, Russia

³Institute for Solid State Physics, University of Latvia, Riga, Latvia

(Received 31 August 2013; published 17 December 2013)

Combining group-theoretical analysis and first-principles density functional theory calculations, we confirm theoretically the antiferrodistortive phase transition in ultrathin SrTiO₃ (001) TiO₂-terminated films and compare it with a similar transition in the bulk. We demonstrate phonon softening at the *M* point of the surface Brillouin zone and analyze the change in the calculated electronic and phonon properties upon phase transition.

DOI: [10.1103/PhysRevB.88.241407](https://doi.org/10.1103/PhysRevB.88.241407)

PACS number(s): 68.47.Gh, 63.22.Kn, 64.60.Bd, 81.90.+c

Incipient ferroelectric strontium titanate SrTiO₃ (STO) serves as a prototype for a wide class of advanced perovskite materials showcasing phenomena such as ferroelectricity,¹⁻³ two-dimensional (2D) electron gas,⁴ or nonvolatile switching memory.⁵ Its bulk properties are well studied, including the antiferrodistortive (AFD) cubic-tetragonal phase transition at 105 K,⁶ which includes *R*-phonon softening with doubling of the unit cell, its elongation in the *z* direction, and alternating rotations of pairs of nearest TiO₆ octahedra in opposite directions. Accordingly, the space group 221, *Pm-3m* (*O_h*¹), changes for space group 140, *I4/mcm* (*D_{4h}*¹⁸). The idea of a similar phase transition at the STO surface or in thin films has a long history (see Refs. 7 and 8), but only very recently a solid experimental proof of this effect was obtained by means of ellipsometric measurements on the STO surfaces.⁹ The studied temperature dependence of the refractive index has shown a jump that is characteristic for second-order phase transitions in the temperature range close to the AFD transition in the STO bulk. Owing to considerable experimental difficulties (including the presence of defects and grain boundaries), very limited reliable information on the AFD surface transitions is available so far in the literature (e.g., the symmetry of surface phonons is not known). Our objective here is to combine a group-theoretical analysis with first-principles calculations in order to shed more light on this effect.

The Landau theory¹⁰ is a commonly used approach for the description of second-order phase transitions, both in triperiodic [three-dimensional (3D)] and diperiodic (2D) systems. It assumes the existence of an order parameter, determined by the components of a vector in the representation space of an irreducible representation (irrep) of the higher-symmetry *G*₀ phase. Hatch and Stokes¹¹ listed all the isotropy subgroups *G* ≤ *G*₀ which leave a partial density distribution function $\rho = \rho_0 + \Delta\rho$ invariant (ρ_0 is invariant under *G*₀, and $\Delta\rho$ denotes the contribution to ρ which appears for nonzero order parameters). The isotropy subgroup *G* is defined for the μ th irrep of *G*₀, given that the μ th irrep of the *G*₀ subduces the identity irrep of *G*. The Landau theory and group-theoretical analysis indicate that the observed AFD phase transition in a 3D case (where *G*₀ is space group 221, and *G* is space group 140) is caused by a softening of the *R*₄₊ phonon mode. Recently we have successfully reproduced this effect in first-principles calculations.¹²

Here we apply the isotropy group formalism to the investigation of the phase transition for the STO surface. We consider the (001) surface of cubic STO (the most stable among the other low-index surfaces)¹³ by means of nonpolar TiO₂-terminated symmetric slabs, consisting of five planes (Fig. 1). We study the TiO₂ termination because (i) it was predominantly studied experimentally (see, e.g., Table 1 in Ref. 13), (ii) it is stronger perturbed with respect to the bulk (i.e., it shows a much larger change in the surface band gap compared to the SrO termination)¹⁴ and thus is expected to show the surface-induced effects, and (iii) the distortion of the TiO₅ semi-octahedra at the surface clearly manifests the 2D effect. We study the five-layer slab for the following reasons: (i) We are interested in a comparison of pure surface effects with the bulk case.¹² (ii) Such ultrathin insulating films are widely investigated both theoretically and experimentally (e.g., to establish a critical film thickness still possessing ferroelectricity¹⁵ and to elaborate on the transport properties of nanoscopic heterostructures).¹⁶ (iii) This study extends our previous one¹⁷ and serves as a basis for researching the charge carrier confinement effects in thin perovskite films.

The symmetry of the considered slabs is described by the diperiodic (layer) group *P4/mmm* (61). The atomic occupation of the Wyckoff positions is given in Table I (1*a*, 2*c*, 2*d*, 2*e* and 4*f* are occupied), as well as the phonon symmetry for these Wyckoff positions. The phonon symmetry of the slab is defined by the symmetry points of a 2D Brillouin zone (BZ) for a square lattice, $\Gamma(0,0)$, $M(\frac{1}{2}, \frac{1}{2})$, and $X(\frac{1}{2}, 0)$. These points are the projections of the 3D BZ symmetry points $\Gamma(0,0,0)$, $R(\frac{1}{2}, \frac{1}{2}, \frac{1}{2})$, $X(\frac{1}{2}, 0, 0)$, and $M(\frac{1}{2}, \frac{1}{2}, 0)$. The site-symmetry approach¹⁸ allows us to find the full mechanical representation of the 3D (2D) periodic system using the induced representations of the space (layer) group and occupation of the Wyckoff positions. The 2D groups' irrep labels are the same as used in Ref. 19 for the space groups, as the layer group *P4/mmm* (61) is a subgroup of space group *P4/mmm* (123), corresponding to a slab of cubic STO (see the 2D-3D group mapping in Table 11.1 in Ref. 20).

In our calculations we used a basis set of linear combination of atomic orbitals (LCAOs) with *d* exponents on Sr, Ti, and O and the PBE0 hybrid exchange-correlation functional in density functional theory (DFT) (to overcome the problem of the underestimated band gap in STO). We employed the CRYSTAL09 computer code²¹ (see the details on the basis sets

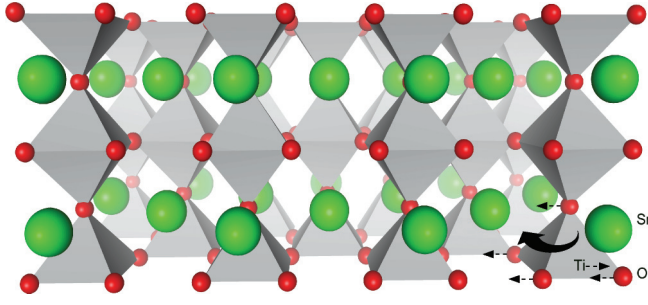


FIG. 1. (Color online) (001) TiO_2 -terminated five-plane slab of STO. The displacement patterns of the imaginary phonon modes at the Γ and M points are shown for a single semioctahedron with dashed and solid arrows, respectively.

and calculation setup in our previous study, Ref. 12, page 4). We calculated the phonon frequencies within the harmonic approximation using the direct frozen-phonon method (displacement magnitude 0.006 \AA). The atomic structure and unit cell parameters of a five-layer freestanding slab (cut off from the cubic bulk crystal) were preliminarily optimized to find the minimum of the total energy. The optimization criteria (root mean square) were 0.00015 and 0.00060 a.u. for the atomic coordinate gradients and the displacements, respectively. As a result, the optimized in-plane lattice constants of a freestanding slab were obtained as 3.85 \AA , which is 0.06 \AA smaller than for the bulk. The effects of thermal lattice expansion at temperatures around the AFD transition (105 K) are smaller by an order of magnitude (10^{-3} \AA) and were neglected. The atomic relaxation at the surface is similar to that found in a

TABLE I. Five-plane TiO_2 -terminated (001) STO slab [layer group $P4/mmm$ (61)]: Occupied Wyckoff positions (given in units of square plane lattice vectors) and induced representations, as found using the SITESYMM program (Ref. 19).

	$\Gamma(0,0)$	$M(\frac{1}{2}, \frac{1}{2})$	$X(\frac{1}{2}, 0)$
Sr $2e(\frac{1}{2}, \frac{1}{2} \pm z)$			
$a_1(z)$	$1^+ 3^-$	$2^- 4^+$	$4^+ 3^-$
$e(x, y)$	$5^+ 5^-$	$5^+ 5^-$	$1^+ 1^- 2^+ 2^-$
Ti $1a(000)$			
$a_{2u}(z)$	3^-	3^-	2^-
$e_u(x, y)$	5^-	5^-	$3^- 4^-$
Ti $2d(00 \pm z)$			
$a_1(z)$	$1^+ 3^-$	$1^+ 3^-$	$1^+ 2^-$
$e(x, y)$	$5^+ 5^-$	$5^+ 5^-$	$3^+ 3^- 4^+ 4^-$
O $2c(0\frac{1}{2}0, \frac{1}{2}00)$			
$b_{1u}(z)$	$3^- 4^+$	5^+	$2^- 4^+$
$b_{2u}(y)$	5^-	$1^+ 2^+$	$1^+ 4^-$
$b_{3u}(x)$	5^-	$3^+ 4^+$	$2^+ 3^-$
O $2d(00 \pm z)$			
$a_1(z)$	$1^+ 3^-$	$1^+ 3^-$	$1^+ 2^-$
$e(x, y)$	$5^+ 5^-$	$5^+ 5^-$	$3^+ 3^- 4^+ 4^-$
O $4f(\frac{1}{2}0 \pm z, 0\frac{1}{2} \pm z)$			
$a_1(z)$	$1^+ 3^- 2^+ 4^-$	$5^+ 5^-$	$1^+ 2^- 4^+ 3^-$
$b_1(x)$	$5^+ 5^-$	$1^- 3^+ 2^- 4^+$	$1^- 2^+ 4^+ 3^-$
$b_2(y)$	$5^+ 5^-$	$1^+ 3^- 2^+ 4^-$	$1^+ 2^- 4^- 3^+$

previous study:²² Oxygen ions move above the Ti ions at the surface, which leads to a rumpling of $\sim 1.5\%$ of the lattice constant.

Using Table I, we performed a symmetry classification of phonons, obtained in our first-principles calculations. Taking into account the cubic bulk STO instability that is concerned with the R_{4+} soft mode, we expect an instability of STO (001) due to a softening of the M_{3+} or M_{5+} modes: These irreps of layer group 61 are subdued by irrep R_{4+} of space group 221. To calculate the phonon frequencies at the M point of the 2D BZ, the surface primitive unit cell was doubled with the transformation matrix $(1 \ 1; -1 \ 1)$. Indeed, we have obtained the imaginary M_{3+} mode (Fig. 1) at the M symmetry point of the 2D BZ in a calculated phonon spectrum. The low-symmetry phase corresponding to this phonon softening is described by the layer group $P4/mbm$ (63).¹¹ Thus, we performed an additional structure optimization within the new symmetry constraints of the layer group 63. The obtained structure relaxation corresponds to the octahedral rotation, similar to the bulk case, accompanied with a hardening of the M_{3+} phonon mode until 129 cm^{-1} and a total energy gain of $\sim 3 \text{ meV}$. An estimated rotation angle of the TiO_5 semioctahedra at the surface is $\sim 0.5^\circ$, which is thus less than the TiO_6 octahedra rotation in the bulk.¹²

As follows from our calculated band structure, the phase transition from the (high temperature) cubic to (low temperature) tetragonal phase in the STO bulk changes the indirect ($R \rightarrow \Gamma$) nature of the optical transition to a direct one ($\Gamma \rightarrow \Gamma$).²³ Similarly, the band gap changes from an indirect to a direct one upon the AFD phase transition on the surface, accompanied with a considerable reduction of the surface band gap (by $\sim 1 \text{ eV}$ compared with the bulk, as discussed earlier).¹³

A comparison of the calculated and experimental Raman phonon frequencies for the AFD bulk (space group 140) and surface (layer group 63) of STO is given in Table II. The experimental phonon frequencies are reported at 15 and 10 K for the bulk and surface phase, respectively. In general, there is a good agreement between the calculated and measured frequencies. We found worse agreement between the phonon frequencies with the experiment for the layer group 61 (i.e., at temperatures above the phase transition).

TABLE II. Calculated and experimental Raman-active phonon frequencies (cm^{-1}) [experimental irreps (Ref. 26) were not reported; the closest are taken].

Irrep	Bulk AFD STO		Surface AFD STO		
	Theory	Expt. (Refs. 24 and 25)	Irrep	Theory	Expt. (Ref. 26)
E_g	17	15, 40	E_g	133i	37
A_{1g}	85	48, 52	E_g	48	48
E_g	142	143, 144	A_{1g}	129	129
			A_{1g}	153	147
			E_g	155	162
B_{2g}	157	235, 229	E_g	180	175
			E_g	421	394
E_g	454	460, 447	B_{1g}	439	447
			B_{1g}	517	548

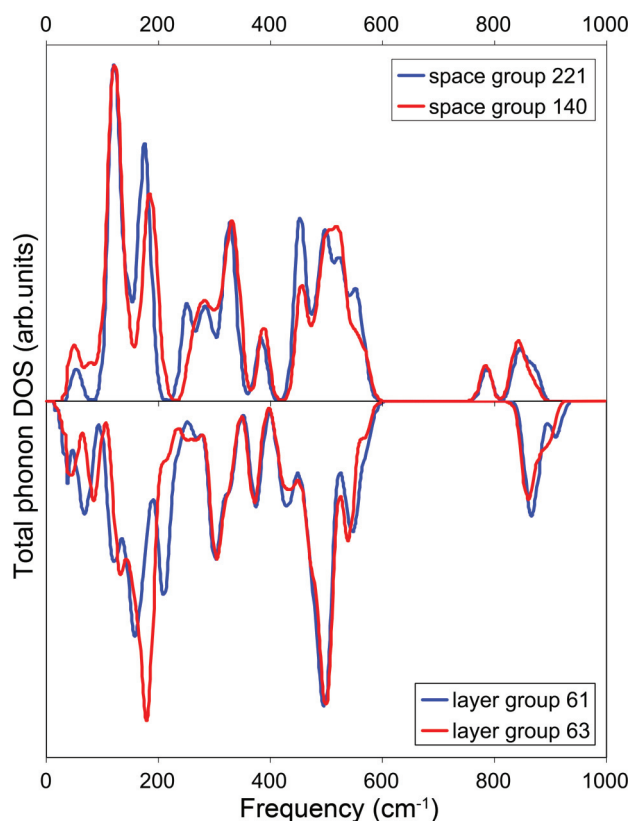


FIG. 2. (Color online) The phonon DOS of bulk (top, 80-atom 3D supercell) and surface (bottom, 26-atom primitive 2D cell) before and after the AFD phase transition (blue and red lines).

In contrast to the bulk AFD phase, the 2D phase shows imaginary frequencies at the Γ point (Γ_{5+} and Γ_{5-} modes, Fig. 1). They are apparently related to the ferroelectric insta-

bility at the STO surface, as discussed earlier in Refs. 27 and 28. Such ferroelectric phase transitions were indeed recently studied experimentally in thin films of incipient ferroelectrics STO and KTaO_3 under in-plane strain produced by different substrates (e.g., Ref. 3). This effect requires further investigation, which, however, lies beyond the scope of this study.

The calculated phonon frequencies were smeared according to a normal distribution (smearing width 10 cm^{-1}), in order to obtain the phonon density of states (DOS, Fig. 2). First, the phonon frequency distribution shows a minor change due to the phase transition, both in the bulk (as we noted in Ref. 12) and at the surface. Second, the peak shifts in the frequency distribution in the vicinity of 100, 180, and 850 cm^{-1} are concerned with the new O vibration patterns allowed in the topmost slab layer.

In conclusion, we have employed both group-theoretical analysis and first-principles hybrid DFT calculations to prove the existence of a second-order AFD phase transition in a defect-free ultrathin film of STO. We have predicted the symmetry of the relevant soft phonon modes and obtained a reduction in the octahedral rotation angle at the surface compared to the bulk case. Calculating the electronic structure of the relaxed surface, we have also ascertained an indirect to direct change of the band gap upon the phase transition, similar to the bulk case. Finally, we have calculated the surface phonon spectrum and found the Raman-active phonon frequencies for the AFD distorted thin film to be in good agreement with available experiments.

The authors are indebted to V. Trepakov and E. Heifets for stimulating discussions and reading the manuscript. E.K. acknowledges support from EC COST project CM 1104, Latvian Grant No. 237/2012, and Stuttgart High Performance Computing Center (project DEFTD).

*Corresponding author: e.blokhin@fkf.mpg.de

¹I. Fedorov, V. Železný, J. Petzelt, V. Trepakov, M. Jelínek, V. Trtík, M. Černánský, and V. Studnička, *Ferroelectrics* **208-209**, 413 (1998).

²A. A. Sirenko, C. Bernhard, A. Golnik, A. M. Clark, J. Hao, W. Si, and X. X. Xi, *Nature (London)* **404**, 373 (2000).

³M. Tyunina, J. Narkilahti, M. Plekh, R. Oja, R. M. Nieminen, A. Dejneka, and V. Trepakov, *Phys. Rev. Lett.* **104**, 227601 (2010).

⁴S. Thiel, C. W. Schneider, L. F. Kourkoutis, D. A. Muller, N. Reyren, A. D. Caviglia, S. Gariglio, J.-M. Triscone, and J. Mannhart, *Phys. Rev. Lett.* **102**, 046809 (2009).

⁵K. Szot, W. Speier, G. Bihlmayer, and R. Waser, *Nat. Mater.* **5**, 312 (2006).

⁶J. F. Scott, *Rev. Mod. Phys.* **46**, 83 (1974).

⁷C. N. W. Darlington and D. A. O. Connor, *J. Phys. C* **9**, 3561 (1976).

⁸J. Prade, U. Schroder, W. Kress, F. W. de Wette, and A. D. Kulkarni, *J. Phys.: Condens. Matter* **5**, 1 (1993).

⁹A. Dejneka, V. Trepakov, and L. Jastrabik, *Phys. Status Solidi B* **247**, 1951 (2010).

¹⁰L. D. Landau and E. M. Lifshits, *Statistical Physics*, 3rd ed. (Pergamon, New York, 1980).

¹¹D. M. Hatch and H. T. Stokes, *Phase Transitions* **7**, 87 (1986).

¹²R. A. Evarestov, E. Blokhin, D. Gryaznov, E. A. Kotomin, and J. Maier, *Phys. Rev. B* **83**, 134108 (2011).

¹³E. Heifets, S. Piskunov, E. A. Kotomin, Y. F. Zhukovskii, and D. E. Ellis, *Phys. Rev. B* **75**, 115417 (2007).

¹⁴E. Heifets, R. Eglitis, E. A. Kotomin, J. Maier, and G. Borstel, *Surf. Sci.* **513**, 211 (2002).

¹⁵D. D. Fong, G. B. Stephenson, S. K. Streiffer, J. A. Eastman, O. Auciello, P. H. Fuoss, and C. Thompson, *Science* **304**, 1650 (2004).

¹⁶N. Nata and J. Maier, *Nature (London)* **408**, 946 (2000).

¹⁷E. A. Kotomin, V. Alexandrov, D. Gryaznov, R. A. Evarestov, and J. Maier, *Phys. Chem. Chem. Phys.* **13**, 923 (2011).

¹⁸R. A. Evarestov and V. P. Smirnov, *Site Symmetry in Crystals: Theory and Applications*, Springer Series in Solid State Sciences Vol. 108, 2nd ed. (Springer, Berlin, 2007).

¹⁹M. Aroyo, A. Kirov, C. Capillas, J. M. Perez-Mato, and H. Wondratschek, *Acta Crystallogr. A* **62**, 115 (2006).

²⁰R. A. Evarestov, *Quantum Chemistry of Solids: First-Principles Treatment of Crystals and Nanostructures*, Springer Series in Solid State Sciences Vol. 153, 2nd ed. (Springer, Berlin, 2012).

- ²¹R. Dovesi, V. R. Saunders, C. Roetti, R. Orlando, C. M. Zicovich-Wilson, F. Pascale, B. Civalleri, K. Doll, N. M. Harrison, I. J. Bush, Ph. D'Arco, and M. Llunell, *CRYSTAL09 User's Manual* (University of Torino, Torino, Italy, 2009).
- ²²E. Heifets, R. I. Eglitis, E. A. Kotomin, J. Maier, and G. Borstel, *Phys. Rev. B* **64**, 235417 (2001).
- ²³E. Heifets, E. Kotomin, and V. A. Trepakov, *J. Phys.: Condens. Matter* **18**, 4845 (2006).
- ²⁴P. A. Fleury, J. F. Scott, and J. M. Worlock, *Phys. Rev. Lett.* **21**, 16 (1968).
- ²⁵J. Petzelt, T. Ostapchuk, I. Gregora, I. Rychetsky, S. Hoffmann-Eifert, A. V. Pronin, Y. Yuzyuk, B. P. Gorshunov, S. Kamba, V. Bovtun, J. Pokorny, M. Savinov, V. Porokhonsky, D. Rafaja, P. Vanek, A. Almeida, M. R. Chaves, A. A. Volkov, M. Dressel, and R. Waser, *Phys. Rev. B* **64**, 184111 (2001).
- ²⁶D. A. Tenne, I. E. Gonenli, A. Soukiassian, D. G. Schlom, S. M. Nakhmanson, K. M. Rabe, and X. X. Xi, *Phys. Rev. B* **76**, 024303 (2007).
- ²⁷N. Bickel, G. Schmidt, K. Heinz, and K. Müller, *Phys. Rev. Lett.* **62**, 2009 (1989).
- ²⁸H. W. Jang, A. Kumar, S. Denev, M. D. Biegalski, P. Maksymovych, C. W. Bark, C. T. Nelson, C. M. Folkman, S. H. Baek, N. Balke, C. M. Brooks, D. A. Tenne, D. G. Schlom, L. Q. Chen, X. Q. Pan, S. V. Kalinin, V. Gopalan, and C. B. Eom, *Phys. Rev. Lett.* **104**, 197601 (2010).